Traveling-wave solutions to thin-film equations

Stefanella Boatto,[1,2] Leo P. Kadanoff,[1,3] and Piero Olla[1,3]
[1]*The James Franck Institute, The University of Chicago, 5640 South Ellis Avenue, Chicago, Illinois 60637*
[2]*Geophysics Department, The University of Chicago, Chicago, Illinois 60637*
[3]*Computational and Applied Mathematics Program, Ryerson Laboratory, The University of Chicago, Chicago, Illinois 60637*
(Received 24 May 1993)

Thin films can be effectively described by the lubrication approximation, in which the equation of motion is $h_t+(h^n h_{xxx})_x=0$. Here h is a necessarily positive quantity which represents the height or thickness of the film. Different values of n, especially 1, 2, and 3 correspond to different physical situations. This equation permits solutions in the form of traveling disturbances with a fixed form. If u is the propagation velocity, the resulting equation for the disturbance is $uh_x=(h^n h_{xxx})_x$. Here, quantitative and qualitative solutions to the equation are presented. The study has been limited to the intervals in x where the solutions are positive. It is found that transitions between different qualitative behaviors occur at $n=3$, 2, $\frac{3}{2}$, and $\frac{1}{2}$. For example, if u is not zero, solitonlike solutions defined on a finite interval are only possible for $n<3$. More specific results can be obtained. In the case in which the velocity is zero, solitons occur for $n<2$. For $n=1$, the region $\frac{3}{2}<n$ is characterized by the presence of advancing-front solutions, with support on $(-\infty,t)$. For $n>\frac{1}{2}$, single-minimum solutions diverging at $\pm\infty$ are possible. The generic solution, present for all positive values of n, is a receding front, which diverges at finite x for $n<0$.

PACS number(s): 47.15.Hg, 47.55.Dz

I. INTRODUCTION

In a series of recent papers [1–4,6] the motion of a thin film of height h has been studied in a one-dimensional geometry so that h depends on one space variable x and the time t. The resulting dynamics is modeled by the equation

$$h_t+(h^n h_{xxx})_x=0\ ,\quad x,t\in\mathbf{R}\ , \tag{1}$$

in which h is required to be positive. Equation (1) arises in several fluid dynamics problems in which inertia is negligible and the dynamics is governed by the presence of viscosity and capillarity forces. In the Hele-Shaw cell [1], the liquid present in a fluid droplet is sucked in such a way as to produce a long thin bridge between two masses of fluids. Under appropriate conditions, the geometry of this problem can be approximated as one dimensional and Eq. (1), for $n=1$, with h the thickness of the bridge, will describe the dynamics of the process. In the spreading of a droplet over a solid surface under the effect of viscosity and capillarity, again the same equation, this time with the parameter n set equal to three, is the one that governs the dynamics [4]. Variations on the same problem are obtained by playing with the boundary conditions at the interface solid fluid. The reason for this is that $n=3$, which corresponds to no-slip boundary conditions, would lead to infinite viscous dissipation [5]. Typically $n=2$, corresponding to a boundary layer of fixed thickness, and $n=1$, corresponding to a thickness $l\sim 1/h$, are the two cases that are considered for $h\to 0$; the case $n=1$ in particular arises when considering a drop on a porous surface [6].

The main difficulty in studying Eq. (1) is its singular behavior for $h=0$. One outstanding question is whether zeros develop in finite time starting with a regular initial condition. What is known is that with periodic boundary conditions, for $n>3.5$ this does not occur [7], while for $n<\frac{3}{2}$ the solution develops zeros in a finite time [3]. One way of looking at the problem has been to study similarity solutions to (1). Bernis, Peletier, and Williams [8] have considered similarity solutions in the form $h(x,t)=t^{-\alpha}H(xt^{-\alpha})$. In this paper we concentrate on solutions which are waves of fixed form traveling to the right,

$$h(t,x)=H(\eta(t,x))\ ,\quad \eta=x-ut\ . \tag{2}$$

With this restriction, Eq. (1) may be integrated in the form

$$H^n H_{\eta\eta\eta}=uH+J\ . \tag{3}$$

Here, J has the physical significance of a current and u is the propagation velocity of the solution. In this paper we focus on the case in which J and u have the same sign and upon regions in which H is greater than zero. In the next section, we see that under these assumptions, we can get a quite complete classification of the possible forms of the $H-\eta$ curves. This section also contains a local analysis which gives a classification of power-law singularities in $H(\eta)$. Section III of this paper treats situations in which either J or u is zero. In these situations one can reduce the equation for H to a pair of first-order equations for the slope and the curvature of $H(\eta)$. Section IV describes flows in the slope-curvature plane for this situation. We show that the local analysis exhausts the possible singularities of $H(\eta)$ and define the possible behaviors as a function of n. Finally, the last section returns to the

case in which both J and u are nonzero, and describes the types of solutions which are possible in this more general case.

II. ANALYSIS OF H VERSUS η SINGULARITIES

Let us assume that u and J are both non-negative. We assume that H is greater than or equal to zero throughout the region of interest. In addition, we take n greater than zero, and consequently H can have only zeros, not infinities, for finite values of η.

Under these assumptions, the qualitative structure of the solution is very simple. Because $H_{\eta\eta\eta}$ must be positive then $H_{\eta\eta}$ can only have at most one zero in the interior of the solution region and is a monotone increasing function of η. It follows that H can have at most two extrema in the interior of the solution region. The two possible extrema are a maximum for smaller η followed by a relative minimum for larger η. Alternatively, there may be one or no extrema. Notice that as one proceeds to the right of any minimum in H, the slope and curvature will both grow. Consequently, to the right of any minimum, we must have H going to infinity. Correspondingly, to the left of any maximum one must have H going to zero, and necessarily at a finite value of η. Also, notice that if H goes to zero as η becomes infinite, then H will be zero (which is permitted) or negative (forbidden) everywhere. Hence, under the stated conditions, all nonzero solutions to Eq. (3) take one of the following forms.

Soliton. A solution in which H is nonzero in a finite interval as shown in Fig. 1(a). This solution can only have a single maximum and no other extrema. For later reference we divide the curve into two regions, each with a specified sign of the slope. These are denoted as s_1 and s_1.

Advancing. A solution like that shown in Fig. 1(b).

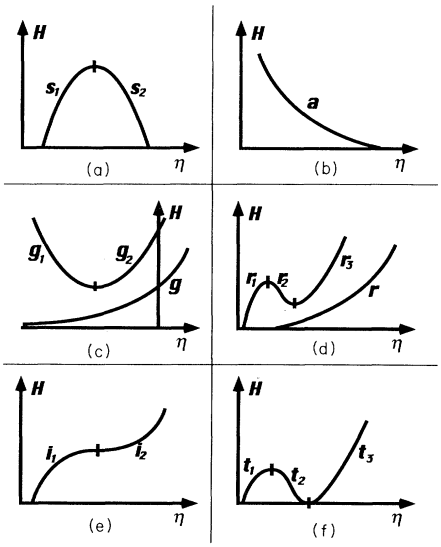

FIG. 1. The types of H *versus* η curves which arise for $r > -3$. (a) shows a soliton solution, (b) an advancing solution, (c) global ones, (d) retreating pattern, (e) an inflection solution, and (f) a solution which touches down and then arises again.

The word "advancing" is used because the fluid advances into the dry region. Such an advancing solution must have H going to infinity as η decreases toward minus infinity.

Global. A solution in which H is positive for all η. In one case, it has a single minimum and diverges at both plus and minus infinity as depicted in Fig. 1(c). There are two types of global solution, one with a minimum, labeled g_1 and g_2, the other of which goes to zero at η equal to minus infinity.

Receding. Solutions like those shown in Fig. 1(d) are also possible. These two kinds of solutions have, respectively, no extrema, or two extrema.

Inflection. Intermediate between the two solution types of Fig. 1(d). This is a solution with one inflection point and no other extrema, as depicted in Fig. 1(e). This serves as a separatrix and is unstable against changes in parameters.

Touchdown. Another unstable separatrix is a curve which just touches down at $H=0$ and rises again.

There are two cases in which we can obtain full information about solutions to Eq. (3). These are situations in which one of the two terms on the right-hand side of Eq. (3) vanish. Then, this equation reduces to

$$H^{3p-1}H_{\eta\eta\eta}=1 \tag{4}$$

after a rescaling. These cases differ in their values of p. If $J=0$ or if J is much smaller than uH, then

$$p=n/3 \quad \text{for } J=0\ . \tag{5a}$$

In the second situation, which is the generic situation as H goes to zero, the height term is negligible and the current term dominates in the right-hand side of Eq. (3). After a change of scale in η, the equation can be reduced to the form (4) with

$$p=(n+1)/3 \quad \text{for } u=0\ . \tag{5b}$$

Our job is to delineate which forms of H *versus* η curves are possible and generic in different regions of p. However, this problem has a more symmetrical solution when the answer is expressed in terms of the alternative parameter r which is related to p by

$$r=4p-3\ . \tag{6}$$

Equation (4) has an exact solution for the two cases $p=\frac{1}{3}$ and 0 corresponding, respectively, to $r=-\frac{5}{3}$ and -3. In those cases one has the explicit solutions

$$H=\begin{cases}\eta^3/6+a\eta^2+b\eta+c\ , & r=-\frac{5}{3} \qquad (7a)\\ ae^{\eta}+b\cos(\sqrt{3}\eta/2+c)e^{-\eta/2}\ , & r=-3\ . \qquad (7b)\end{cases}$$

For $r=-\frac{5}{3}$ one has a cubic curve which can have solitonlike form, and receding fronts of both types and an inflection solution like that shown in Fig. 1(e). There are no advancing fronts and no global solutions. For $r=-3$, a global solution in which H goes to zero on the left also becomes possible. [Take a to be positive and $b=0$ in Eq.

(7b).] This global solution and the inflection solution [which appears in both (7a) and (7b)] are unstable in that a small change in parameters can completely destroy the solution or change its character. The remaining solution types in Eq. (7) are stable against all small changes of parameters.

We shall be interested in the character of the zeros and infinities of H, since the nature of these singularities will determine much of the character of the time dependence emerging from Eq. (1) [3]. In particular, a matching of powers implies that there are three possible forms of zeros or infinities of H. The three cases are that, for η going to zero or infinity, we can have solutions in the form:

$$H \simeq \begin{cases} a|\eta|^{1/p} \quad (N) & (8a) \\ a\eta + b\eta^{4-3p} \quad (L) & (8b) \\ a\eta^2 + b\eta^{5-6p} \quad (Q) \ . & (8c) \end{cases}$$

Here, L and Q stand for linear and quadratic while N describes a situation in which the power is generically a noninteger. [In the N case, Eq. (8a) gives an exact solution when a is correctly chosen.] For Eq. (8a), the condition that a must be positive determines the sign of η. For the N solution to be positive, we must have r in the range

$$-3 < r < -1 \text{ or } r > 1 \ , \quad (N) \quad \eta > 0 \tag{9a}$$

$$r < -3 \text{ or } -1 < r < 1 \ , \quad (N) \quad \eta < 0 \ . \tag{9b}$$

The L and Q solutions are obtained as an asymptotic expansion in η. In Eq. (8) the first term on the right of the equal sign is the leading-order result, with the next term being a small correction. Then, these expansions give zeros or infinities of H according to the rule

$$r < 1 \Longrightarrow H \to 0 \ , \quad r > 1 \Longrightarrow H \to \infty \ , \quad (L) \tag{10a}$$

$$r < -1 \Longrightarrow H \to 0 \ , \quad r > -1 \Longrightarrow H \to \infty \ , \quad (Q) \ . \tag{10b}$$

Thus, for example, the $r = -\frac{5}{3}$ case, with the solution given in Eq. (7a), always has H going to infinity via the N solution which then implies that the infinity only occurs when η goes to positive infinity. Thus, the demands of Eq. (9) are satisfied. Equations (10) are also fulfilled since both linear and quadratic zeros may occur but not linear or quadratic infinities.

The remaining cases are the boundary cases in which $r = -3$, $r = -1$, or $r = 1$. The first case is described by Eq. (7b). In the second case, the quadratic and the N singularities merge while in the third the linear and N-type singularities merge. These latter two cases give new singularity types:

$$\ln H \simeq 2\ln\eta + 2/3 \ln|\ln\eta| + \cdots$$

$$\text{for } \eta \to +\infty \text{ or } \eta \nearrow 0 \ , \quad (NQ) \ r = -1 \tag{11a}$$

$$\ln H \simeq \ln|\eta| + 1/3 \ln|\ln|\eta|| + \cdots$$

$$\text{for } \eta \to -\infty \text{ or } \eta \searrow 0 \ , \quad (NL) \ r = 1 \ . \tag{11b}$$

Equations (8)–(11) describe how zeros and infinities may occur in H via behaviors which asymptote to simple power laws. More complex behaviors are possible in which it is proportional to a power but also has some oscillatory structure in it. We shall have more to say about these behaviors in the next section in which we replace the equation for H by a pair of first-order ordinary differential equations for the slope S and the curvature, C of $H(\eta)$. In this representation these "oscillatory" singularities will correspond to limit cycles in the C-S plane. After a bit of analysis, we shall argue that the limit cycles do not exist so that Eqs. (8)–(11) exhaust the possible singularities in $H(\eta)$.

III. MAIN FEATURES OF THE C-S PLANE

We can do a much more general analysis of Eq. (4). First notice that (4) is invariant under the rescaling

$$H \to aH \ , \quad \eta \to a^p \eta \ . \tag{12}$$

From any solution to (4) we can get another solution by doing a rescaling in the form given by Eq. (12). Another way of generating a new solution is the displacement of η by a fixed amount. When these invariances are taken into account, the solutions of Eq. (4) become a one-parameter family of essentially different solutions.

There is a standard device for making use of invariances like these. Whenever the independent variable does not appear in the set of equations one can lower the order of the differential equation by expressing it as an equation for the derivative of the independent variable in terms of the independent variable itself [9]. Here, we use the following change of variables, which both lowers the order of the equation and eliminates any explicit dependence upon the new independent variable $\ln H$:

$$S(H) = H^{p-1} H_\eta \ , \quad \frac{d}{d\eta} = \frac{S}{H^p} \frac{d}{d\ln H} \ . \tag{13}$$

Equation (4) then becomes the second-order equation

$$S[SS'' + (p-1)(2p-1)S^2 + (3-4p)SS' + S'^2] = 1 \ ;$$

$$S' = \frac{dS}{d\ln H} \ . \tag{14}$$

Here and below we use primes to denote derivates with respect to $\ln H$. We could at this point change variables to lower the order once again. Instead, we choose to use the change of variables to obtain a first-order autonomous system for a pair of variables S and a new variable related to the curvature

$$C(S) = \frac{S'}{S} = \frac{H_{\eta\eta} H}{H_\eta^2} + p - 1 \ . \tag{15}$$

Thus, we can replace Eq. (13) by the pair of statements:

$$C' = V_C(C,S) = (1/S^3) - 2C^2 + rC + (1-r^2)/8 \ , \tag{16a}$$

$$S' = V_S(C,S) = CS \ . \tag{16b}$$

In this way, the irrelevant integration constant associated with the similarity property (12) is reabsorbed through the use of logarithmic variables, changing the problem to that of analyzing a pair of first-order nonlinear ordinary

differential equation.

The kind of analysis that will be carried on here will consist of studying the trajectories in the C-S plane of solutions to Eq. (16), and then in understanding the result in terms of H-η variables. In this section we will analyze the asymptotic behavior of solutions of Eq. (4). In the following section we will focus on building up a correspondence between qualitative features of trajectories in the C-S and in the H-η plane.

Notice that Eq. (16) shows a symmetry between the positive and negative domains of r, specifically, (16) is invariant under the replacements: $r \rightarrow -r$, $C \rightarrow -C$ (corresponding to replacing H with $1/H$). Therefore, any analysis we carry out for positive r can be extended immediately to negative r.

Our first step is to locate all the singularities and other significant features of H *versus* η in terms of flows in the C-S plane. The behaviors described in Eqs. (8) and (11) show routes by which H can go to zero or infinity. Indeed, inverting Eq. (13) we obtain

$$H(S)=H(S_0)\exp\left[\int_{S_0}^{S}\frac{dS'}{S'C(S')}\right].$$

This last equation shows that $H \rightarrow 0$ and $H \rightarrow \infty$ at finite S when $SC(S) \rightarrow 0$, which corresponds to the fixed point of Eqs. (16a) and (16b),

$$(C,S)=[0,2(1-r^2)^{-1/3}\ \ (N)\ . \tag{17a}$$

As indicated this fixed point corresponds to H going to zero or infinity via the N route of Eq. (8a). The second possibility is that $S \rightarrow \infty$ along a trajectory in the C-S plane. In this case, the term $(1/S^3)$ in Eq. (16a) can be neglected. If one traces back the origin in this term, one finds that it comes from the one in front of Eq. (4), so that we are solving $H^{3p-1}H_{\eta\eta\eta}=0$, which can have only linear and quadratic solutions. From Eq. (16a),

$$(C,S)=[(r+1)/4\ ,\pm\infty\ ]\ (Q)\ , \tag{17b}$$

$$(C,S)=[(r-1)/4\ ,\pm\infty\ ]\ (L)\ . \tag{17c}$$

The sign of infinity gives the sign of the slope at the singularity. We shall have to investigate the stability of these "fixed points." First, however, notice that the flow can go to two additional boundary fixed points at $S=0$ (indicating zero slope) and C equal to plus or minus infinity. These correspond to extrema of the $H-\eta$ curves with the two types being

$$(C,S)=(-\infty,0)\ \ (\text{maximum})\ , \tag{17d}$$

$$(C,S)=(\infty,0)\ \ (\text{minimum})\ . \tag{17e}$$

The maximum and minimum always form attractive fixed points. The pair of fixed points Q and L have stability properties which depend upon r. These fixed points are at infinite S and at the C values

$$C_{\pm}=(r\pm 1)/4\ . \tag{18}$$

A linear stability analysis about these fixed points shows that in the neighborhood of the fixed points

$$C-C_{\pm}\sim H^{\mp 1}\ , \tag{19a}$$

$$S^{-1}\sim H^{-C_{\pm}}\ . \tag{19b}$$

If both quantities on the right-hand side of (19) go to zero as H approaches its limiting value, then the fixed point will attract all trajectories in its vicinity. Thus, the collection of orbits of this type cover a finite portion of the entire space. These orbits are then said to have codimension zero. If the exponents have opposite sign, there will be two lines of points attracted to the fixed point, but all other orbits in the neighborhood will be repelled. Thus, the fixed point will have one attractive and one repulsive direction. This is a situation in which the orbits cover an infinitesimal fraction of the entire space (sets of measure zero), and in fact, have codimension one. Finally, if both quantities go to infinity, then all possible deviations from the fixed point will lead to trajectories which fail to reach that point. This is a codimension two situation. Thus, if $r>-1$ the quadratic fixed point will be attractive as H goes to infinity. We have already seen that it does not exist for H going to zero. If $r<-1$ the fixed point will describe a zero with one attractive and one repulsive direction. Conversely, the linear fixed point will be an attractive zero for $r<1$ and will have an infinity with attractive and repulsive directions for $r>1$.

The qualitative behavior of the N-type fixed point are only slightly more complex. A linear analysis about the fixed points shows that the deviation for the fixed point grows as H^{β} where the power takes on the values

$$\beta=\frac{r}{2}\pm\left[\frac{3-r^2}{8}\right]^{1/2}\ . \tag{20}$$

This indicates that the fixed point has attractive and repulsive directions for $r^2<1$. In this situation, the orbit is of codimension 1. For $r<-1$ this fixed point is attractive as H goes to infinity and is repulsive (codimension 2) for H going to zero. The converse behavior holds for $r>1$. However, at $r^2=3$ there is a change in behavior because the eigenvalue becomes complex. When $1<r^2<3$ the eigenvalues of the stability matrix are real and all orbits flow directly into the fixed point. When $r^2>3$ the orbits spiral and are either of codimension zero or two.

IV. FLOWS IN THE tanh$C$ – tanh$S$ PLANE

All the remaining qualitative features of solutions to Eq. (16) can be obtained by looking at the sign of C' and S' to see the directions of flow C-S plane. In order to fit all regions onto the picture, we actually use the tanh$C$ – tanh$S$ plane. The regions in which the ratio

$$R=\frac{(\tanh C)'}{(\tanh S)'}=\frac{\cosh^2 S}{\cosh^2 C}\left[\frac{1}{CS^4}-\frac{2(C-C_+)(C-C_-)}{CS}\right] \tag{21}$$

are positive or negative are drawn out in Fig. 2 for a par-

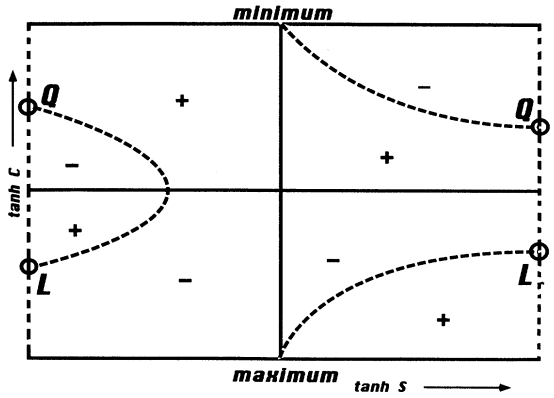

FIG. 2. The regions of different behavior in the tanh$C$–tanh$S$ plane. The signs show whether the $C(S)$ curves have a positive or negative slope. The dashed lines have slope zero, the solid ones slope infinity. The different kinds of fixed points are labeled and described. This figure describes the situation when $-1<r<1$.

ticular case in which $-1<r<1$. The plus signs indicate positive regions, the minus signs indicate negative regions, the light lines zeros of the ratio, and the heavy lines infinities. The lines intersect at the fixed points discussed above. The N fixed point is given by Eq. (16a). Note that C' is zero at

$$S(C)=2[(C-C_+)(C-C_-)]^{-1/3} . \tag{22}$$

Here, $C_\pm$ are the values of C at the two fixed points Q and L. These fixed points are also drawn in Fig. 2. They are labeled to show the behavior of H in their neighborhood.

Any trajectory $C(S)$ must be an increasing function in the sectors of the plane labeled by a + and a decreasing one in those labeled by −. These trajectories never cross the axis $S=0$ at finite C, since this would correspond to a nonquadratic extremum, with $H_{\eta\eta\eta}=0$ and $H\neq 0$, which, for $p\neq 0$, is forbidden by Eq. (4).

Now we are in a position to draw out the trajectories in this plane. This is done in Fig. 3. There is one feature in Fig. 3 which is far from obvious. The question is the following: should we have included limit cycles in our drawing of the possible trajectories? Any limit cycle will give a singularity in $H(\eta)$. Notice that most types of limit cycles are impossible. No limit cycle can go across the line at $S=0$ since we know that there may be no more than two crossings of this line. Hence, we confine our considerations to flows which stay on one side of that boundary. To have a limit cycle, one must have a flow which is topologically equivalent to the one shown in Fig. 4. This configuration occurs only around the N fixed point, when $|r|>1$. Consequently, any limit cycle must encircle that fixed point and stay completely within the right half-plane.

To eliminate the possibility of these cycles we look back at Eq. (16) which implies that all trajectories in the C-S plane obey the orbit equation

$$\frac{1}{2}\frac{d(C^2S^4)}{dS}=1+rS^3C+\frac{1-r^2}{8}S^3 . \tag{23}$$

Imagine that we have a limit cycle. Integrate (23) about that cycle to find

$$\oint dS\, S^3Cr=0 . \tag{24}$$

For $r\neq 0$, Eq. (24) is quite impossible since $C(S)dS$ will

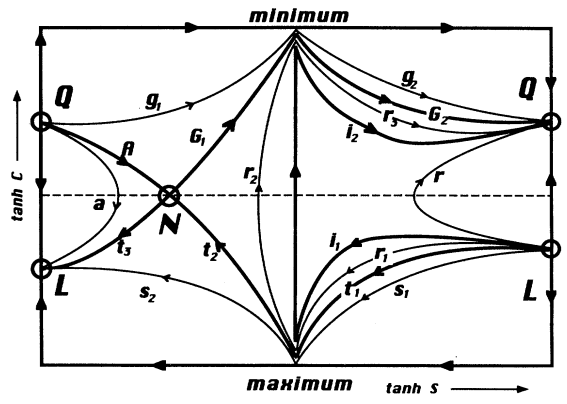

FIG. 3. Orbits in the tanh$C$–tanh$S$ plane. The heavy curves are separatrices; the light ones generic orbits. The different kinds of fixed orbits are labeled. The arrows show the direction of flow when η is increasing. This figure describes the situation when $-1<r<1$.

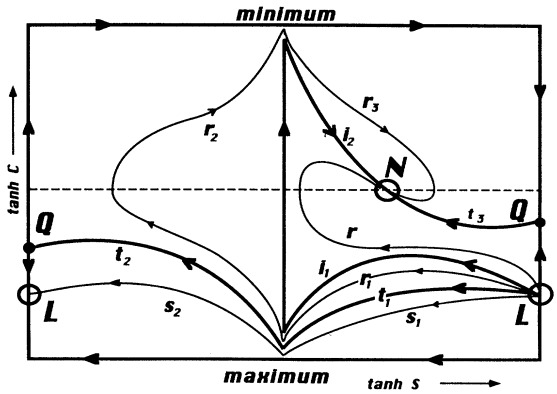

FIG. 4. Orbits in the tanh$C$–tanh$S$ plane. The same as Fig. 3 except that these orbits are now drawn for the case in which $-\sqrt{3}<r<-1$.

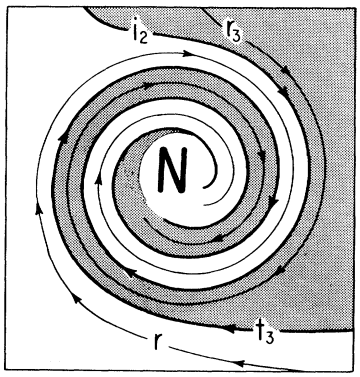

FIG. 5. Spiral near the N fixed point for $r<-\sqrt{3}$. Different regions of the picture correspond to different regions of global behavior: trajectories lying in the shaded region correspond to retreating solutions with two local extrema, while those which lie outside of it correspond to simple retreating solutions.

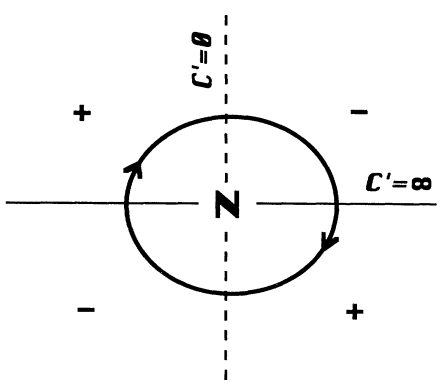

FIG. 6. How the topology around the N fixed point could lead, for $|r|>1$, to the presence of a limit circle; plus and minus signs correspond again to trajectory slopes. In order to exclude this possibility, information about the precise form of the relation $C=C(S)$ is required. For $|r|<1$, the slope signs are switched, leading to hyperbolic trajectories.

always be positive in any portion of the loop. [An exact solution, see Eq. (26) below, eliminates the possibility of loops for $n=0$.] Therefore we do not have any limit cycle. The rest of the analysis of the flow is quite straightforward. Notice that the boundaries of the plane and the S axis are automatically trajectories. We put arrows on all trajectories to show the direction of increasing η. The sign of S_η is the same as the sign of C. Therefore the trajectories take the form shown schematically in Fig. 3. We have distorted the region near the maximum and minimum to show the connection among the different trajectories. Actually, all trajectories in the neighborhood of these points pass through the boundary fixed points shown. The heavier trajectories shown serve as separatrices and are exceptional. The lighter ones have the same form as all the other trajectories in their neighborhoods. All the lighter trajectories have the form shown in the first four parts of Fig. 1. Separatrices of the touchdown and inflection form also appear. The touchdown separatrix passes through the N fixed point. At this point, H osculates the η axis. The two curves labeled G_1-G_2 and A have not been described previously. They are, respectively, global and advancing solutions. For this special advancing solution H osculates the η axis as an N-type zero. For the exceptional global solution, H goes to infinity but, since the infinity occurs at the N fixed point, H goes to infinity more weakly than for any of the other trajectories.

The results of Figs. 2 and 3 can be checked by considering a situation in which an exact solution for the trajectories is possible. Take $r=0$, then Eq. (16) gives an equation for $C(S)$ which is

$$S\frac{d}{dS}(C^2/2)=\frac{1}{S^3}-2(C^2-\tfrac{1}{16}) \tag{25}$$

which then has the general solution

$$C^2=\frac{1}{16}-\frac{2}{3S^2}+\frac{u}{S^4}\ . \tag{26}$$

The different trajectories are labeled by the constant of

TABLE I. The orbit types for $-1<r<1$.

Singularity at left			Intermediate behavior	Singularity at right			
H	η	type	orbit	H	η	type	Codimension
0	finite	L	r	∞	∞	Q	0
0	finite	L	$r_1r_2r_3$	∞	∞	Q	0
0	finite	L	s_1s_2	0	finite	L	0
∞	$-\infty$	Q	a	0	finite	L	0
0	finite	L	t_1t_2	0	finite	N	1
∞	$-\infty$	N	t_3	0	finite	L	1
0	finite	L	i_1i_2	∞	∞	Q	1
∞	$-\infty$	N	a	0	finite	N	2

TABLE II. The orbit types for $-3 < r < -1$.

Singularity at left			Intermediate behavior	Singularity at right			
H	η	type	orbit	H	η	type	Codimension
0	finite	L	r	∞	∞	N	0
0	finite	L	$r_1 r_2 r_3$	∞	∞	N	0
0	finite	L	$s_1 s_2$	0	finite	L	0
0	finite	L	$t_1 t_2$	0	finite	Q	1
0	finite	Q	t_3	∞	∞	N	1
0	finite	L	$i_1 i_2$	∞	∞	N	1
0	finite	L	r	∞	∞	N	2

TABLE III. The orbit types for $r = -1$.

Singularity at left			Intermediate behavior	Singularity at right			
H	η	type	orbit	H	η	type	Codimension
0	finite	L	r	∞	∞	NQ	0
0	finite	L	$r_1 r_2 r_3$	∞	∞	NQ	0
0	finite	L	$s_1 s_2$	0	finite	L	0
0	finite	L	$t_1 t_2$	0	finite	NQ	1
0	finite	L	$i_1 i_2$	∞	∞	NQ	1

TABLE IV. The orbit types for $r > 1$.

Singularity at left			Intermediate behavior	Singularity at right			
H	η	type	orbit	H	η	type	Codimension
0	finite	N	r	∞	∞	Q	0
0	finite	N	$r_1 r_2 r_3$	∞	∞	Q	0
∞	$-\infty$	Q	$g_1 g_2$	∞	∞	Q	0
0	finite	N	r	∞	∞	L	1
0	finite	N	$i_1 i_2$	∞	∞	Q	1
∞	$-\infty$	L	$g_1 g_2$	∞	∞	Q	1

TABLE V. The orbit types for $r = 1$.

Singularity at left			Intermediate behavior	Singularity at right			
H	η	type	orbit	H	η	type	Codimension
0	finite	NL	r	∞	∞	Q	0
0	finite	NL	$r_1 r_2 r_3$	∞	∞	Q	0
∞	$-\infty$	Q	$g_1 g_2$	∞	∞	Q	0
0	finite	NL	$i_1 i_2$	∞	∞	Q	1
∞	$-\infty$	NL	$g_1 g_2$	∞	∞	Q	1

TABLE VI. Generic singular behaviors for $u>0$ and $J>0$. All infinities occur at $\eta=\pm\infty$. All zeros occur at finite η. The L's and Q's permit zeros or infinities for both directions of increase of η. However, for the N's the zeros and infinities can either occur on the left or the right of the solution region, as shown.

Case	Possible infinities	Possible zeros
$n\geq 2$	Q	N (on left)
$\frac{3}{2}<n<2$	Q	L
$0<n\leq\frac{3}{2}$	$N(\eta\rightarrow\infty)$	L

integration u. The inflection curve has $u=0$ while 3 gives the trajectories which pass through the N fixed point. Note that, as stated above, Eq. (26) does not permit limit cycles.

We summarize the results of the analysis for $-1<r<1$ by presenting, in Table I, a listing of the different kinds of orbits observed. The last column in the table gives the codimension of the orbit, i.e., the number of boundary conditions which must be precisely set in order to achieve an orbit of the given kind.

The same kind of analysis can be applied in the other regions of r. For example, for $-\sqrt{3}<r<-1$, the trajectories in the plane take the form shown in Fig. 4. Once again, the light curves are generic and the dark ones are separatrices. The labels correspond exactly to the curves listed in Fig. 1. When $-3<r<-\sqrt{3}$, there is only a change in detail. The N fixed point gains complex eigenvalues and thence becomes a spiral. Then in the neighborhood of the fixed point, there is a complex pattern (see Fig. 5) or orbits of type i, r, t, and r_3. Thus, there is a sensitivity to initial data in this region. A comparison with the exact solution (7b) shows why this is reasonable. In that case there are oscillations which die away as η goes to infinity. Nonetheless, it is the tiny remnant of these oscillations which determine how a set of boundary conditions in the region of large η will produce the observed (and different) behaviors for smaller η. Table II lists the orbit types in this range of r.

Figure 6 shows the behavior that arises in the boundary case $r=-1$ in which the N and Q fixed points merge. In this case, the touchdown curve loses its t_3 segment. Otherwise, all the curves are of the types we have described heretofore. The curve types are summarized in Table III.

The analysis for the other cases is exactly the same as the one we have already given. We show in Table IV the orbit types for $r>1$. For $r>\sqrt{3}$ the motion in the neighborhood of the N fixed point once again shows a spiral structure, so one has a kind of sensitive dependence upon initial conditions. The case $r=1$ is described in Table V. Here the N and L fixed points have merged so that orbit structure is simplified.

TABLE VII. Generic solutions for $Ju>0$.

Case	Solitons	Global solution	Advancing front	Receding front
$n\geq 2$	No	Yes	No	Yes
$\frac{3}{2}<n<2$	Yes	Yes	Yes	Yes
$n\leq\frac{3}{2}$	Yes	No	No	Yes

TABLE VIII. Generic solutions for $Ju<0$.

Case	Solitons	Global solution	Advancing front	Receding front
$n\geq 2$	No	Yes	Yes	No
$\frac{3}{2}<n<2$	Yes	Yes	Yes	Yes
$n\leq\frac{3}{2}$	Yes	No	No	Yes

V. CONCLUSIONS

In the general case, Eq. (3) shows that J and u are both nonzero. Naturally, the J term will dominate the behavior as H goes to zero while the u term will dominate as h goes to infinity. If the signs of u and H are different one term can work against the other, and a variety of new phenomena might arise. However, if the signs are the same, the analysis we have used up to now will describe the general nature of the orbits. The only difference is that one uses Eq. (5a) to estimate the p value for infinities and Eq. (5b) to estimate the p value for zeros. Once again, we keep to the case $n>0$. Using the results from Tables I–V leads, therefore, to the generic behaviors in the case $u>0$ and $J>0$ as cited in Table VI. The solutions of type N become of type NL and NQ, respectively, at $n=\frac{3}{2}$ and $n=3$. Changing the sign of u and J changes the direction in η in which the corresponding singularity occur. Although the analysis carried on in this paper does not apply in the intermediate region in which both terms on the right-hand side of Eq. (3) are of the same order, the results from the table above allow to derive conclusions on which solutions are definitely not allowed in the various ranges of n. In Tables VII and VIII, the "yes" cases are allowed, provided one assumes that the asymptotic behaviors can be matched freely. In the case that u and J have the same sign, one obtains, therefore, the results cited in Table VII. When u and J have opposite sign, one finds instead the results cited in Table VIII. However, the reader should notice that the "no" in Table VIII is less definitive than the "no" in Table VII. If J and u have apposite signs, limit cycles might occur and they might give rise to new kinds of singularities.

ACKNOWLEDGMENTS

We would like to thank Andrea Bertozzi, Michael Brenner, and Todd Dupont for interesting and helpful conversations. This research was supported in part by the University of Chicago Material Research Laboratory.

[1] P. Constantin, T. F. Dupont, R. E. Goldstein, L. P. Kadanoff, M. Shelley, and S. Zhou, Phys. Rev. E **47**, 4169 (1993).
[2] M. Brenner and A. Bertozzi, Phys. Rev. Lett. **71**, 593 (1993).
[3] A. Bertozzi, M. Brenner, T. Dupont, and L. Kadanoff, *Applied Mathematics Series Centennial Volume* (Springer-Verlag, Berlin, in press).
[4] H. Greenspan, J. Fluid Mech. **84**, 125 (1978).
[5] E. B. Dussan V. and S. Davis, J. Fluid Mech. **173**, 115 (1986).
[6] P. Neogi and C. A. Miller, J. Colloid Interface Sci. **92**, 460 (1976).
[7] F. Bernis and A. Friedman, J. Diff. Eq. **83**, 179 (1990); L. P. Kadanoff (unpublished).
[8] F. Bernis, L. A. Peletier, and S. M. Williams, *Nonlinear Analysis Theory, Methods and Applications* (Pergamon, New York, 1992), Vol. 18, p. 217.
[9] C. M. Bender and S. A. Orszag, *Advanced Mathematical Methods for Scientists and Engineers* (McGraw-Hill, New York, 1978).